Thermal induced changes on the properties of spin-coated P3HT:C_{60} thin films for solar cell applications

David E. Motaung[1, 2], Gerald F. Malgas[1,*], Christopher J. Arendse[1], Sipho E. Mavundla[1, 3] Clive J. Oliphant [1, 2] and Dirk Knoesen[2]

[1]National Centre for Nano-structured Materials, Council for Scientific Industrial Research, P. O. Box 395, Pretoria, 0001, South Africa
[2]Deparment of Physics, University of the Western Cape, Private Bag X17, Bellville, 7535, South Africa
[3]Deparment of Chemistry, University of the Western Cape, Private Bag X17, Bellville, 7535, South Africa

ABSTRACT

The thermal transition behaviour, optical and structural properties of spin-coated P3HT:C_{60} blended films with different C_{60} ratios were investigated using differential scanning calorimetry (DSC), thermo-gravimetric analysis (TGA), ultraviolet-visible (UV-Vis) spectroscopy, photoluminescence (PL), Fourier transform infrared absorption (FT-IR) spectroscopy and Raman spectroscopy. DSC analysis showed that the P3HT:C_{60} blends have quite different thermal characteristics. The absorption spectra of the annealed P3HT:C_{60} (1:1 wt. %) films becomes enhanced and red shifted. This feature is evident in the photoluminescence measurements where the formation of polymer crystallites upon annealing is observed. Raman spectroscopy showed a substantial ordering in the polymer film during annealing. It was found that the performance of a P3HT:C_{60} (1:1 wt. %) device was dramatically improved by annealing.

Keywords: poly(3-hexylthiophene), optical properties, annealing, thermal transition

---

* Corresponding Author: Dr. Gerald Malgas, Tel: (+27) 012 841 3972,
Fax: (+27) 012 841 2229, Email: gmalgas@csir.co.za

1. INTRODUCTION

During the last decade, plastic solar cells have attracted substantial research interest because of their advantageous properties, such as low cost, light weight, large-area fabrication and mechanically flexible [1-7]. The main focus in the organic solar cell research lies on increasing the power conversion efficiency under simulated sunlight [8]. It has been reported that by using high mobility donor polymers (e.g. poly(3-hexylthiophene) (P3HT)) and fullerene derivative, phenyl-C_{61}-butyric acid methyl ester (PCBM), as an electron acceptor yield a power conversion efficiencies (PCEs) of 5% [8-10]. Recently, PCE of up to 6.5% were reached for tandem cells [11]. Apart from the power conversion efficiency, there is however at least two other important factors that will put organic solar cells one step closer to commercialisation, such as processing into large area modules [5, 7, 12-13] and long-term stability of devices [13-22]. The production of very large area plastic solar cell modules up to 1000 cm^2 has been reported [5, 7, 13]. This has shown that it is highly feasible with existing technology to mass produce polymer solar cells at a very low cost.

Studies on the stability of organic photovoltaic cells have typically focussed on optimisation of the stability of encapsulated devices under continuous light illumination [13-15, 18-20]. Brabec et al. [20] reported lifetimes of up to 2000 h continuous operation for devices protected from oxygen and water ingress. However, lifetimes of up to 6000 h were achieved with an entirely flexible encapsulation technology [13]. Krebs et al. [14, 15]

2

found a stable polymer solar cell with a lifetime of up to 10000 h with the careful exclusion of water and oxygen. They also predicted an operational lifetime in excess of 20 000 h by using a thermal acceleration factor of 4 between 25 and 72 °C and an indoor illumination in tensities of 50-100 W m^{-2}. It has been reported that ITO/ZnO/ZnO:poly-(3-carboxydithiophene) (P3CT)/PEDOT:PSS/Ag inverted type solar cells without sealing maintained 80 % of the initial performance for continuous illumination for 100 h in an ambient atmosphere [21]. In spite of tremendous advances in both the understanding and fabrication of organic solar cells, operational stability has reached a lifetime up to a year under outside conditions [17, 23]. These studies on the stability/degradation [13-22] issues; showed that the topic is rather complicated and not fully understood.

Among conjugated polymers, poly(3-alkylthiophenes) (P3ATs) are one of the most promising conducting polymers because of their interesting electronic and optical properties and also because of their processability and chemical stability. Recently, semi crystalline regioregular poly(3-hexylthiophene) (P3HT) has attracted a lot of attention as a donor material, as it has the highest charge carrier mobility among the conjugated polymers and an absorption edge around 650 nm (band gap of 1.9 - 2.0 eV), combined with a high hole mobility exceeding 0.1 cm^2/Vs [24]. These qualities make P3HT a good candidate for the polymer in polymer photovoltaic cells [8, 25–26]. In this paper, the thermal transition behaviour, structural and optical properties of P3HT:C$_{60}$ films with different blends are investigated at different annealing temperatures.

2. EXPERIMENT DETAILS

2.1 Sample preparation

All the chemicals used in this experiment were purchased from Sigma Aldrich. A regio-regular poly (3-hexylthiophene) (RR-P3HT) polymer was used as a light absorption and electron donating material; while a C_{60} fullerene was used as an electron acceptor material. These materials were used as received, without further purification. Indium tin oxide (ITO) coated on a 1 mm glass substrate with a resistance between 8 and 12 Ω/square, was successively cleaned with solvents and dried in dry nitrogen. A mixture of rr-P3HT (5 mg) and C_{60} with different ratios (2.5 mg, 5 mg, 20 mg) was dissolved in 1mL of chloroform solution. The solution was stirred over night at 50 °C in order to mix the P3HT:C_{60} solution completely. A thin layer of poly (3,4-ethylenedioxythiophene):poly (styrenesulfonate) (PEDOT:PSS) solution was spin coated onto the ITO glass substrates and onto silicon (Si) substrates with the spin rate of 2500 rpm for 30 s. This was followed by thermal treatment of the substrates at 100 °C for 30 min.

The P3HT:C_{60} blend with a thickness of about 100 nm was spin coated onto the PEDOT:PSS layer. The spinning rate and time of spin-coating were 2500 rpm and 30 s, respectively. However, for some samples no poly(3,4-ethylenedioxythiophene)-polystyrene sulphonic acid (PEDOT:PSS) layer was deposited onto the ITO/Glass and Si substrates. The samples were dried on a hot plate at a temperature of 50 °C for 15 min. The thermal annealing procedure was accomplished by placing the P3HT:C_{60}/ITO/Glass or P3HT:C_{60}

/Si structures in an oven at different temperatures ranging from 85 - 150 °C for a period of 30 min.

2.2 Characterization

The absorption spectra of the P3HT:C_{60} organic layers with different ratios taken before and after the annealing procedure were measured by a Perkin Elmer UV/VIS spectrometer from 900 to 300 nm. The photoluminescence (PL) spectra were measured by exciting the samples with 350 nm line of deuterium lamp. It should be noted that for some photoluminescence and Raman measurements, that the blends deposited onto Si (100) substrates were used. The PEDOT:PSS/ITO glass substrates was not used in order to avoid masking of P3HT features which overlap with those of PEDOT. The emission was detected with Jobin Yvon PMT detector. The structure of pure P3HT with different concentrations of C_{60} was characterized by Fourier transform infrared spectroscopy (FT-IR) using a Perkin Elmer FT-IR spectrometer and Raman spectroscopy using a Horiba Jobin Yvon HR800 micro-Raman spectrometer. The Raman spectroscopy measurements were conducted at room temperature with a 514 nm excitation laser. It should also be noted that for some FTIR and Raman spectroscopy measurements that the blends were spin-coated on a Si (100) substrate. The films thickness was measured using a Veeco DEKTAK 6M Stylus profilometer. Differential scanning calorimetry (DSC) curves for P3HT, C_{60} and the two different P3HT:C_{60} blends were obtained with a TA Q2000 DSC. Approximately 7 mg of each sample was loaded in an aluminium pan. The analyses were conducted from -50 °C to 250 °C at heating and cool ing rates of 10 °C /min

5

and a nitrogen flow rate of 5 mL/min. Thermo-gravimetric analysis (TGA) (stability measurements) was performed on the two different P3HT:C_{60} blends using a TA Q500 thermogravimetric analyser. Measurements were carried out in an oxygen atmosphere at a heating rate of 10 °C /min from room temperature to 950°C.

Solar cells were completed by evaporating 100 nm of Al on top of the active layer. The current–voltage (IV) characteristics were measured using a Keithley 2420 and a solar simulator equipped with a xenon short arc lamp with a power of 150 W and an AM 1.5G solar filter. The influence of thermal annealing on the photovoltaic performance was measured after the samples were annealed.

3. RESULTS AND DISCUSSION

3.1. *Differential scanning calorimetry (DSC)*

The thermal behaviour of P3HT and blends of P3HT:C_{60} (1:1 wt. %) and P3HT:C_{60} (1:4 wt. %) have been studied by DSC analysis. Figure 1 shows the differential scanning calorimetry (DSC) measurements of P3HT and its blends heated from -50 °C to 250 °C in a nitrogen gas at a flow rate of 5 mL min^{-1}. It is evident from the cooling curves (Fig. 1(a)) that an endothermic transition is centred at 199.9 °C in regioregular P3HT and with a glass transition (T_g) $\approx$ -4.7 °C. Zhao et al. [27] reported that during a non-isothermal experiment that at a slower cooling rate, the crystallization of P3HT would start at higher temperatures, quite slowly and then continue over a wide temperature range. The transition shows the typical features of a

melting/crystallization transition. The melting temperature depends on the crystallization conditions. A transition enthalpy value (ΔH=17.5 J/g) was obtained during an exothermic transition from a crystalline to a liquid crystalline state around 229 °C. However, Chen et al. [28] determined a melting temperature of 240–245 °C for head-to-tail regioregular P3HT, while no indication for a glass transition temperature was given.

It is observed that DSC analysis of fullerene has two crystallizations peaks at around -16.6 °C and -15.2 °C (arrow) with a relaxation region at ~ 14.7 °C and an enthalpy of 8.9 J/g (Fig. 1(b)). When the polymer (P3HT) is blended with a C_{60} (1:1 wt. %), as shown in Figure 1 (c), they both exhibits endothermic and exothermic events which shifts to lower temperatures. The shifting of P3HT to lower temperatures is due to an addition of C_{60}. For the P3HT:C_{60} (1:4 wt. %) blend (Figure 1 (d)), it can be seen that P3HT peaks becomes flat (or disappears), indicating that C_{60} fullerene has an effect on the structure of P3HT. A similar behaviour was observed by Cugola et al. [29].

3.2. Thermo-gravimetric analysis (TGA)

To estimate the thermal stability of P3HT:C_{60} with different C_{60} ratios, TGA analysis was performed in an O_2 atmosphere. Figure 2 shows the TGA and differential thermal analysis (DTA) of (a) P3HT:C_{60} (1:1 wt. %) and (b) P3HT:C_{60} (1:4 wt. %) blends. During sample preparation, nearly equal amounts (~7 mg) of the blends were loaded into a platinum pan. It is observed from Figure 2 (a) that the P3HT:C_{60} (1:1 wt. %) mass loss takes place in a two-step mechanism, where the DTA consists of two maxima at temperatures around 454 and 614 ℃. The first step of the mass loss began

at about 430 ℃ and the second step began at about 526 ℃. Such an oxidation at high temperature obviously cannot be due to physisorbed species [30]. The beginning of the mass loss is probably due to the loss of an alkyl side group attached to the aromatic thiophene backbone (hexyl group). As the temperature increases above 500 ℃, the oxidati on is accelerated and the pyrolysis of the aromatic backbone of polymer chains is ignited.

It can be seen from Figure 2(b) that the $P3HT:C_{60}$ (1:4 wt. %) composites exhibit slightly inferior thermal stability with increasing amount of fullerene contents as compared to the $P3HT:C_{60}$ (1:1 wt. %) blend. The first step of the mass loss began at about 420 ℃ and the second step began at about 518 ℃. This may be due to low physico-chemical bonding states and microstructural features of the composites including the branching/percolating. Kumar et al. [31] showed that when P3HT is blended with a high amount of single walled carbon nanotubes (SWCNTs), the thermal stability decreases. Therefore, it can be concluded that the addition of fullerene C_{60} to P3HT reduces the thermal stability of P3HT

3.3. Ultraviolet-Visible Spectroscopy (UV-Vis)

Absorption spectra of mixtures of $P3HT:C_{60}$ with different ratios dissolved in chloroform solution were investigated before and after thermal annealing. Figure 3 shows the UV–Vis spectra measured for as-prepared $P3HT: C_{60}$ (1:1 wt. %) films and that annealed at different temperatures. For the as-prepared film, the maximum peak absorption wavelength is at 502 nm with a shoulder at 600 nm and a barely visible shoulder at 544 nm. The effect of thermal annealing on the absorption spectra is apparent for the films

8

treated at different temperatures. Broadening of the spectra towards longer wavelengths is observed when the annealing temperature increases. After annealing at 110 °C and above, the intensity of absorption peaks increases, λ_{max} is at 513 nm, showing a red shift, and the shoulders at 546 nm and 605 nm become more distinguishable.

The film annealed at 150 °C shows a similar behaviour as the one annealed 110 °C, this clearly a superposition of the two spectra. Similar results were obtained for the P3HT:C_{60} (1:4 wt. %) blend (results not shown). The absorption shift in the spectra suggests that annealing induced some ordering in the polymer chains. These changes may be attributed to an increasing interchain interaction among P3HT chains. It also indicates strong interchain–interlayer interactions among the P3HT chains as well as good polymer ordering in the blend films **[28, 32-34]**. The increasing interchain interaction among the P3HT chains because of thermal annealing results in more delocalized conjugated π electrons, the lowering of the band gap between π and π^*, and the increase of the optical π–π^* transition which results in the observed red shift in the peak absorption wavelength.

3.4. Photoluminescence (PL)

Photoluminescence measurements on P3HT:C_{60} thin films (Figure 4) provide further evidence of the formation of polymer crystallites. The photoluminescence of the annealed sample is several times higher than that of the as-prepared ones. This indicates that the photo-induced electron transfer from the polythiophene becomes less efficient upon annealing. However, Malgas et al. **[30]** showed that a complete quenching is observed

for a P3HT:C_{60} (1:1 wt. %) composite film without thermal annealing. The efficiency of electron transfer depends obviously on the mean distance between the conjugated polymer and fullerene molecules. If the distance between the polymer and fullerene becomes comparable with the exciton diffusion length (~10 nm), some excitons cannot reach the neighbouring fullerene molecule and recombine radiatively, giving rise to photoluminescence signal. Since the concentration of the C_{60} in the film does not change upon annealing, we conclude that the change of the photoluminescence intensity originates from a phase separation and thus changes in the morphology of the active layer. Furthermore, in agreement with the crystallization process, a polymer aggregate formation is strongly indicated by the observation of a characteristic red shift in the PL spectrum of the annealed sample [35].

3.5. Fourier Transform Infrared Spectroscopy (FT-IR)

The FTIR spectra of rr-P3HT films deposited on a Si substrate and compared with that annealed at different temperatures are shown in Figure 5. The absorption band assignments of the FTIR absorption peaks for rr-P3HT are given in Table 1. The thiophene ring associated with P3HT shows an out of plane deformation of C-H, and the band at 819 cm^{-1} is assigned to this C-H deformation vibration of P3HT. The peak at 1509 and 1457 cm^{-1} represents the antisymmetric C=C stretching and symmetric stretching mode of P3HT, respectively. The ratio between the intensity of the antisymmetric stretching mode at 1509 cm^{-1} and the intensity of the symmetric stretching peak mode at

1456 cm^{-1} can be used to probe the average conjugation length of P3HT **[36, 37]**.

When the P3HT films are annealed at different temperatures, little or no shifts to shorter or longer wavenumbers are observed for the aliphatic-C–H stretching vibrations and the C-H out of plane deformation. However, the intensity of the aliphatic-C–H stretching and aromatic-C-H out plane vibrations increases with an increase in annealing temperature, suggesting that the relative amount of twisting moiety in the crystalline state increases. Street et al. **[38]** reported that annealing induces the reorientation of lamellae and formation of high-mobility percolation paths with low-angle grain boundaries.

3.6. Raman Spectroscopy

Figure 6 compares the Raman spectra of the rr-P3HT films deposited on a Si substrate with that annealed at different temperatures for 30 min. The spectrum of the rr-P3HT film deposited on Si features all the vibrational frequencies expected for the conjugated polymer **[39]**. The peak at 1450 cm^{-1} can be attributed to the symmetric C=C stretching deformation, while the medium intensity band at 1375 cm^{-1} is associated with C–C stretching deformations in the aromatic thiophene ring **[35, 40]**. In order to extract additional information from the Raman spectra, we compared the 1350-1500 cm^{-1} region of P3HT film before and after thermal annealing (insert Figure 6). It is observed that the intensity in the Raman shift of the symmetric C=C mode and C–C mode in the aromatic thiophene ring increases with annealing temperature suggesting a substantial ordering in the polymer film during heating. This is in good agreement with the photoluminescence data. No

11

peak shift are observed in the C=C signal after annealing. A downward shift in the wavenumber generally indicates an increase in the crystallinity of P3HT polymer and the extension of the effective conjugation length along the polymer backbone [41].

3.7. Photovoltaic measurements

A popular strategy to improve the power conversion efficiency with a fixed material system is by post-production annealing. We have carried out the thermal treatment of the devices before the metal (Al) electrode deposition. The dark J–V curves of the P3HT devices with different C_{60} ratios are shown in Fig. 7(a). The conductivities of the P3HT:C_{60} were increased by blending C_{60}. The higher the concentration of $C_{60;}$ the higher the conductivity of P3HT:C_{60} devices. The device performance for as-prepared and annealed photovoltaic devices of the type ITO/P3HT:C60 (1:1 wt. %)/Al under AM1.5 conditions with light intensity of 1000W/m^2 at room temperature are shown in Figure 7(b). Improvements of the photovoltaic characteristics are observed during annealing in Figure 7 and Table 2. The short-circuit current density and fill factor increased for the higher temperature annealed (150 °C) device, leading to an improvement of power conversion efficiency going from η= 0.009 % for the as-prepared device to η = 0.029 % for the 150°C annealed sample; suggesting that carrier transport network in the cells was promoted. However, the open-circuit voltage decreases upon annealing. It has been demonstrated that in polyalkylthiophenes the improvement of three dimensional ordering/conjugation is leading to lower oxidation potentials [42].

12

Therefore the increase of polymer ordering by thermal annealing (also observed by UV-vis and Raman spectroscopy), may account for the drop-off of V_{oc}.

4. CONCLUSION

We have studied the structural and optical properties of both as-prepared and annealed P3HT:C_{60} blended films using, DSC, TGA, UV–Vis absorption, photoluminescence, FT-IR, and Raman spectroscopy. DSC analysis showed that the blends have quite different thermal properties. TGA thermographs showed that the P3HT:C_{60} composites exhibit a slightly inferior thermal stability with an increased amount of fullerene. A red shift of the absorption was found for annealed P3HT:C_{60} (1:1 wt. %) films. These changes were explained in terms of the formation of polymer crystallites upon annealing. The photoluminescence measurements confirmed the formation of the polymer crystallites upon annealing and also showed that the photo-induced electron transfer becomes less effective upon annealing. This concludes that the degree of order in the polymer films has a drastic effect on both the absorption properties and the electron charge transport. It was found that the performance of a P3HT:C_{60} device improved by annealing.

5. AKNOWLWDGEMENTS

6. REFERENCES

[1]   C. J. Brabec, N. S. Sariciftci, J. C. Hummelen, Plastic solar cells, Adv. Funct. Mater. 11 (2001) 15-26.

[2]   H. Spanggaard, F. C. Krebs, A brief history of the development of organic and polymeric photovoltaics, Sol. Energy Mater. Sol. Cells 83 (2004) 125-146.

[3]   C. Winder, N. S. Sariciftci, Low bandgap polymers for photon harvesting in bulk heterojunction solar cells, J. Mater. Chem. 14 (2004) 1077-1086.

[4]   E. Bundgaard, F. C. Krebs, Low band gap polymers for organic photovoltaics, Sol. Energy Mater. Sol. Cells 91 (2007) 954-985.

[5]   F. C. Krebs, J. Alstrup, H. Spanggaard, K. Larsen, E. Kold, Production of large-area polymer solar cells by industrial silk screen printing lifetime consideration and lamination with polyethyleneterephthalate, Sol. Energy Mater. Sol. Cells 83 (2004) 293-300.

[6]   S. Günes, H. Neugebauer, N. S. Sariciftci, Conjugated polymer-based organic solar cells, Chem. Rev. 107 (2007) 1324-1338.

[7]   F. C. Krebs, H. Spanggaard, T. Kjaer, M. Biancardo, J. Alstrup, Large area plastic solar cell modules, Mater. Sci. Eng. B 138 (2007) 106-111.

[8]   F. Padinger, R. S. Rittberger, N. S. Sariciftci, Effects of postproduction treatment on plastic solar cells, Adv. Funct. Mater. 13 (2003) 85-88.

[9]   W. Ma, C. Yang, X. Gong, K. Lee, A. J. Heeger, Thermally stable, efficient polymer solar cells with nanoscale control of the interpenetrating network morphology, Adv. Funct. Mater. 15 (2005) 1617-1622.

[10] G. Li, V. Shrotriya, J. Huang, Y. Yao, T. Moriarty, K. Emery, Y. Yang, High-efficiency solution processable polymer photovoltaic cells by self-organization of polymer blends, Nat. Mater. 4 (2005) 864-868.

[11] J. Y. Kim, K. Lee, N. E. Coates, D. Moses, T. Q. Nguyen, M. Dante, A. J. Heeger, Efficient tandem polymer solar cells fabricated by all-solution processing, Science, 317 (2007) 222-225.

[12] G. Dennler, C. Lungenschmied, H. Neugebauer, N. S. Sariciftci, A. Labouret, Flexible, conjugated polymer-fullerene-based bulk-heterojunction solar cells: basics, encapsulation, and integration, J. Mater. Res. 20 (2005) 3224-3233.

[13] C. Lungenschmied, G. Dennler, H. Neugebauer, N. S. Sariciftci, M. Glatthaar, T. Meyer, A. Meyer, Flexible long-lived, large-area, organic solar cells, Sol. Energy Mater. Sol. Cells 91 (2007) 379-384.

[14] F. C. Krebs, H. Spanggaard, Significant improvement of polymer solar cell stability, Chem. Mater. 17 (2005) 5235-5237.

[15] F. C. Krebs, K. Norrman, Analysis of the failure mechanism for a stable organic photovoltaic during 10,000 h of testing, Prog. Photovolt.: Res. Appl. 15 (2007) 697-712.

[16] X. Yang, J. Loos, S. C. Veenstra, W. J. H. Verhees, M. M. Wienk, J. M. Kroon, M .A. J. Michels, R. A. J. Janssen, Nanoscale morphology of high-performance polymer solar cells, Nano Lett. 5 (2005) 579-583.

[17] E. A. Katz, S. Gevorgyan, M. S. Orynbayev, F. C. Krebs, Out-door testing and long-term stability of plastic solar cells, Eur. Phys. J. Appl. Phys. 36 (2007) 307-311.

[18]   H. Neugebauer, C. J. Brabec, J. C. Hummelen, N. S. Sariciftci, Stability
       and photodegradation mechanisms of conjugated polymer/fullerene
       plastic solar cells, Sol. Energy Mater. Sol. Cells 61 (2000) 35-42.

[19]   F. Padinger, T. Fromherz, P. Denk, C. J. Brabec, J. Zettner, T. Hierl, N.
       S. Sariciftci, Degradation of bulk heterojunction solar cells operated in
       an inert gas atmosphere: a systematic study, Synth. Met. 121 (2001)
       1605-1606.

[20]   C. J. Brabec, J. A. Hauch, P. Schilinsky, C. Waldauf, Production
       aspects of organic photovoltaics and their impact on the
       commercialization of devices, MRS Bull. 30 (2005) 50-53.

[21]   F. C. Krebs, Air stable polymer photovoltaics based on a process free
       from vacuum steps and fullerenes, Sol. Energy Mater. Sol. Cells 92
       (2008) 715-726.

[22]   M. Jørgensen, K. Norrman, F. C. Krebs, Stability/degradation of
       polymer solar cells, Sol. Energy Mater. Sol. Cells 92 (2008) 686-714.

[23]   J. A. Hauch, P. Schilinsky, S. A. Choulis, R. Childers, M. Biele, C. J.
       Brabec, Flexible organic P3HT:PCBM bulk-heterojunction modules with
       more than 1 year outdoor lifetime, Sol. Energy Mater. Sol. Cells 92
       (2008) 727-731.

[24]   D. H. Kim, Y. D. Park, Y. S. Jang, H. C. Yang, Y. H. Kim, J. I. Han, D.
       G. Moon, S. J. Park, T. Y. Chang, C. W. Chang, M. K. Joo, C. Y. Ryu,
       K. W. Cho, Enhancement of field-effect mobility due to surface-
       mediated molecular ordering in regioregular polythiophene thin film
       transistors, Adv. Func. Mater. 15 (2005) 77-82.

[25] N. Camaioni, G. Ridolfi, G. C. Miceli, G. Possamai, M. Maggini, The effect of a mild thermal treatment on the performance of poly(3-allkylthiophene)/fullerene solar cells, Adv. Mater. 14 (2002) 1735-1738.

[26] I. Riedel, V. Dyakonov, Influence of electronic transport properties of polymer-fullerene blends on the performance of bulk heterojunction photovoltaic devices, Phys. Status. Solidi. (a) 201 (2004) 1332-1341.

[27] Y. Zhao, G. Yuan, P. Roche, M. Leclerc, A calorimetric study of the phase transitions in poly(3-hexylthiophene), Polymer, 36 (1995) 2211-2214.

[28] T-A. Chen, X. Wu, D. Rieke, Regiocontrolled synthesis of poly(3-alkylthiophenes) mediated by Rieke Zinc: their characterization and solid-state properties, J. Amer. Chem. Soc. 117 (1995) 233-244.

[29] R. Cugola, U. Giovanella, P. Di Gianvincenzo, F. Bertini, M. Catellani, S. Luzzati, Thermal characterization and annealing effects of polythiophene/fullerene photoactive layers for solar cells, Thin Solid Films 511-512 (2006) 489-493.

[30] G. F. Malgas, C. J. Arendse, S. Mavundla, F. R. Cummings, Interfacial analysis and properties of regioregular poly(3-hexylthiophene) spin-coated on an indium tin oxide-coated glass substrate, J. Mater. Sci. 43 (2008) 5599-5604.

[31] J. Kumar, R. K. Singh, V, Kumar, R.C. Rastogi, R. Singh, Self-assembly of SWCNT in P3HT matrix, Diamond Rel. Mater. 16 (2007) 446-453.

[32] R. D. McCullough, S. Tristram-Nagle, S. P. Williams, R. D. Lowe, M. Jayaraman, Self-orienting head-to-tail poly(3-alkylthiophenes): new insights on structure-property relationships in conducting polymers, J. Amer. Chem. Soc. 115 (1993) 4910-4911.

[33] H. Sirringhaus, N. Tessler, R.H. Friend, Integrated optoelectronic devices based on conjugated polymers, Science 280 (1998) 1741-1744.

[34] H. Sirringhaus, P.J. Brown, R.H. Friend, M.M. Nielsen, K. Bechgaard, B.M.W. Langeveld-Voss, A.J.H. Spiering, R.A.J. Janssen, E.W. Meijer, P. Herwig, D.M. de Leeuw, Two-dimensional charge transport in self-organized, high-mobility conjugated polymers, Nature 401 (1999) 685-688.

[35] P. J. Brown, D. S. Thomas, A. Kohler, J.S. Wilson, J.-S. Kim, C.M. Ramsdale, H. Sirringhaus, R. H. Friend, Effect of interchain interactions on the absorption and emission of poly(3-hexylthiophene), Phys. Rev. B 67 (2003) 064203-064218.

[36] Y. Furukawa, M. Akimoto, I. Harada, Vibrational key bands and electrical conductivity of polythiophene, Synthetic Met. 18 (1987) 151-156.

[37] M. Trznadel, A. Pron, M. Zagorska, R. Chrzaszcz, J. Pielichowski, Effect of molecular weight on spectroscopic and spectroelectrochemical properties of regioregular poly(3-hexylthiophene), Macromolecules 31 (1998) 5051-5058.

[38] R. A. Street, J. E. Northrup, A. Salleo, Transport in polycrystalline polymer thin-film transistors, Phys. Rev. B 71 (2005) 165202-165214.

[39] R. Osterbacka, C. P. An, X. M Jiang, Z. V. Vardeny, Delocalized polarons in self-assembled poly(3-hexyl thiophene) nanocrystals, Synth. Metal 116 (2001) 317-320.

[40] G. Louarn, M. Trznadel, J. P. Buisson, J. Laska, A. Pron, M. Lapkowski, S.J. Lefrant, Raman spectroscopic studies of regioregular poly(3-alkylthiophenes), J. Phys. Chem. 100 (1996) 12532-12539.

[41] C. Heller, G. Leising, G. Godon, S. Lefrant, W. Fischer, F. Stelzer, Raman excitation profiles of conjugated segments in solution, Phys. Rev. B 51 (1995) 8107-8114.

[42] M. Catellani, C. Arbizzani, M. Mastragostino, A. Zanelli, Poly(3-buthyl-co-3,4dibuthylthiophene)s: synthesis and electrochromic characterization, Synth. Met. 69 (1995) 373-374.

Figure Captions and Tables

Figure 1: DSC curves of **(a)** P3HT, **(b)** fullerene (C_{60}), **(c)** P3HT: C_{60} (1:1 wt. %) and **(d)** P3HT: C_{60} (1:4 wt. %), at heating rates of 10 °C min^{-1} with a nitrogen flow rate of 5 mL min^{-1}.

Figure 2: TGA graphs of **(a)** P3HT:C_{60} (1:1 wt. %), **(b)** 1:4 wt. % and its derivative plot showing the decomposition stages.

Figure 3: Absorption spectra of an as-prepared P3HT:C_{60} (1:1 wt. %) composite film compared with that annealed at different temperatures. The annealing time for all the films was 30 min.

Figure 4: Photoluminescence spectra of **(a)** P3HT:C_{60} (1:1 wt. %) and **(b)** 1:4 wt. %. as-prepared and the annealed films. A considerable increase of the structure and some red-shift is observed, typical for crystalline ordering of the conjugated polymer.

Figure 5: FTIR absorbance spectra of as-prepared rr-P3HT films compared with that annealed at different temperatures for 30 min.

Figure 6: Raman spectra of rr-P3HT film spin-coated on a Si substrate compared with that annealed at different temperatures for 30 min.

Figure 7: Current density–voltage (J–V) characteristics of the (a) P3HT:C_{60} solar cells with different C_{60} ratios in dark and (b) as-prepared and annealed P3HT:C_{60} (1:1 wt. %) devices under white light illumination.

TABLE 1: FTIR band positions (cm^{-1}) and their assignments of P3HT films annealed at different temperatures.

TABLE2: Photovoltaic devices performance of P3HT:C_{60} (1:1 wt. %) structures before and after annealing.
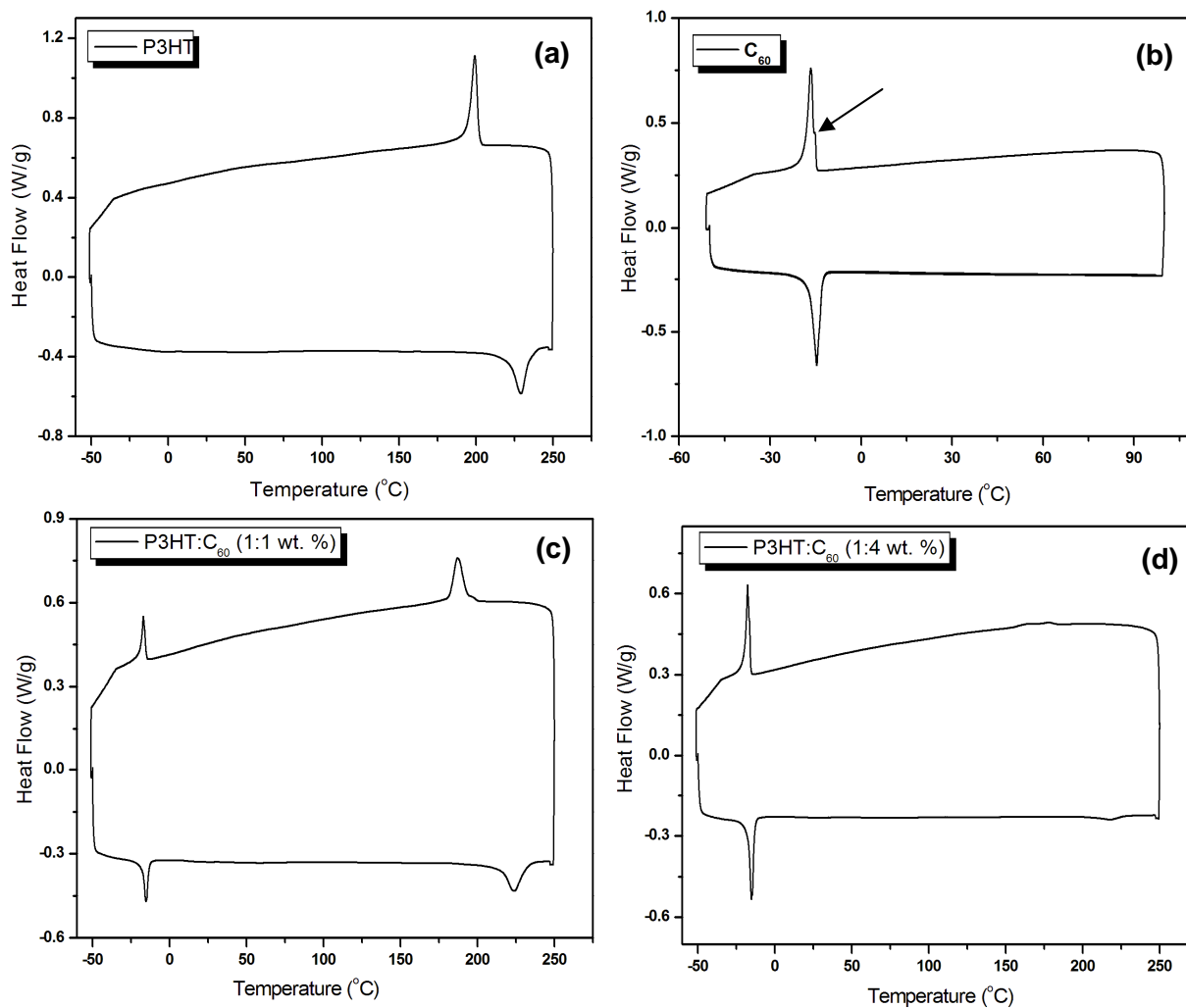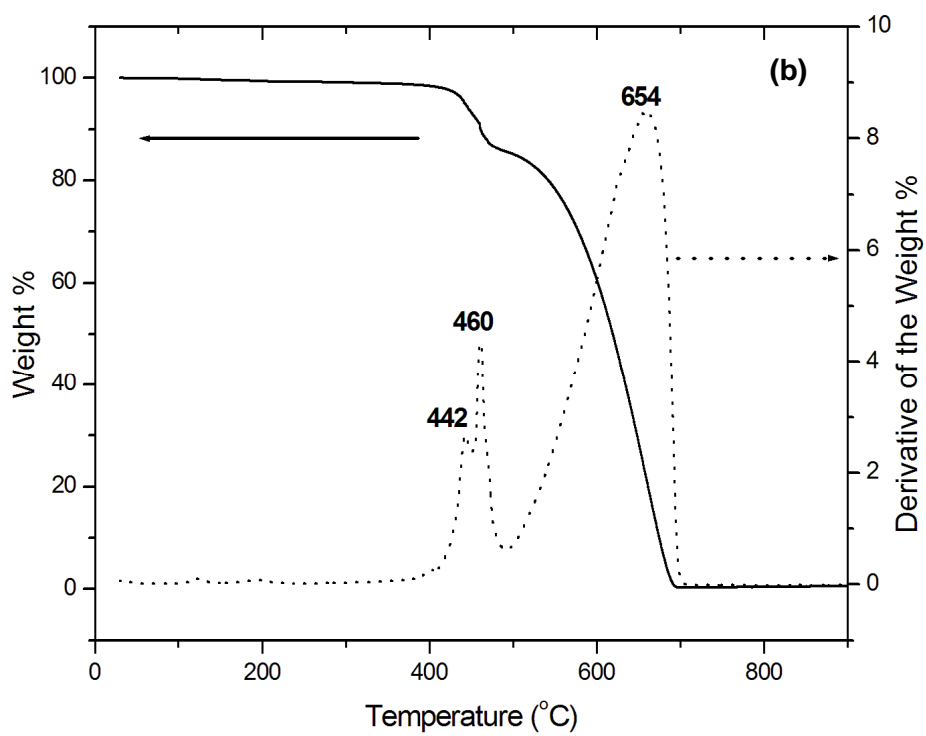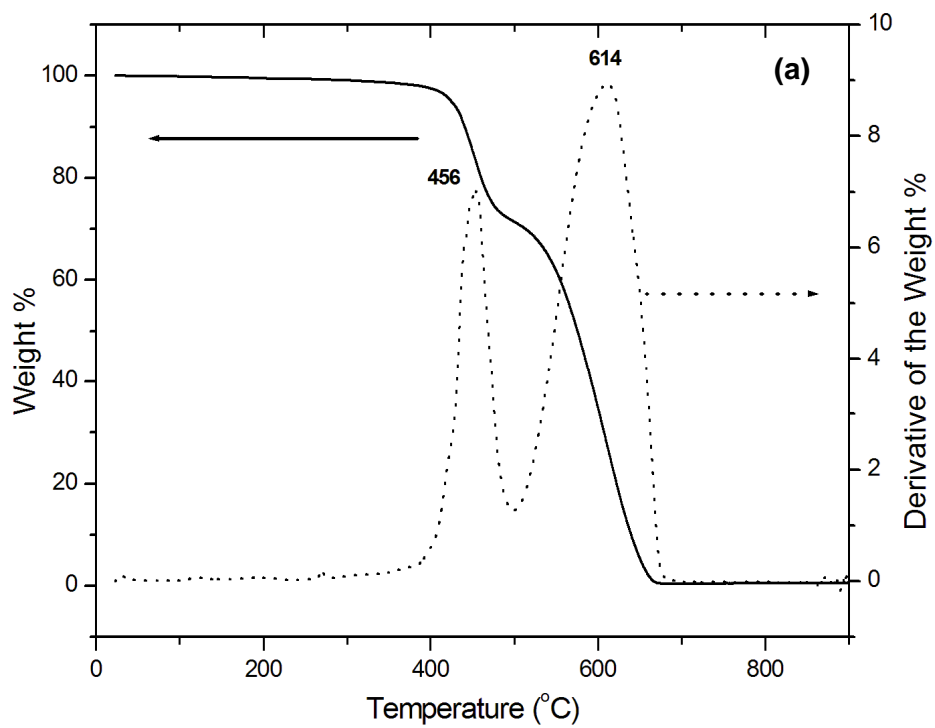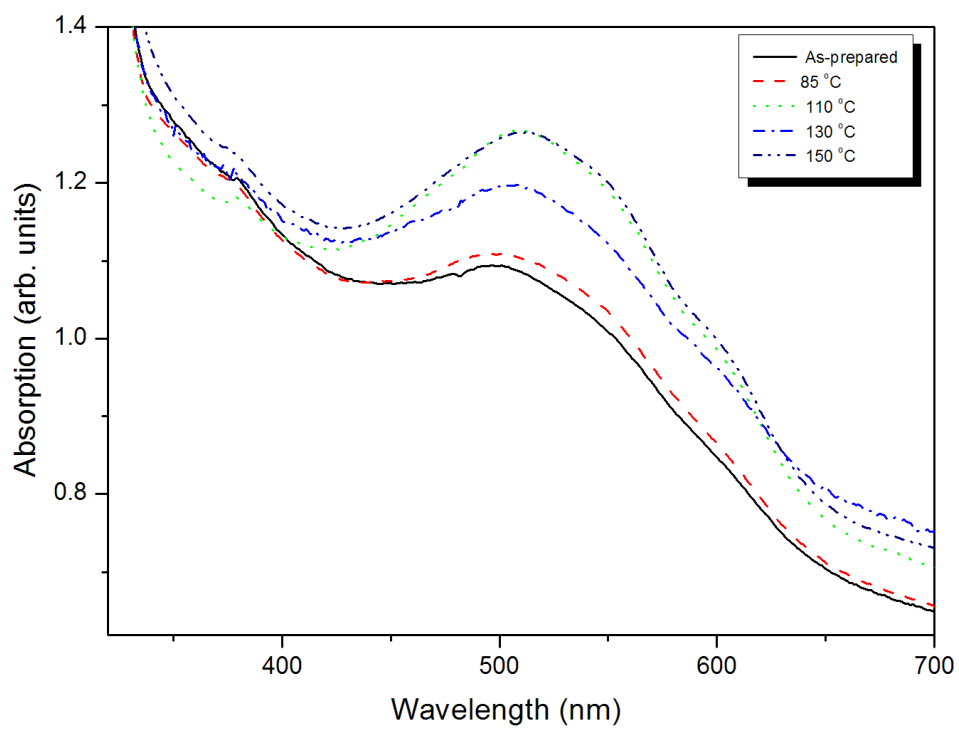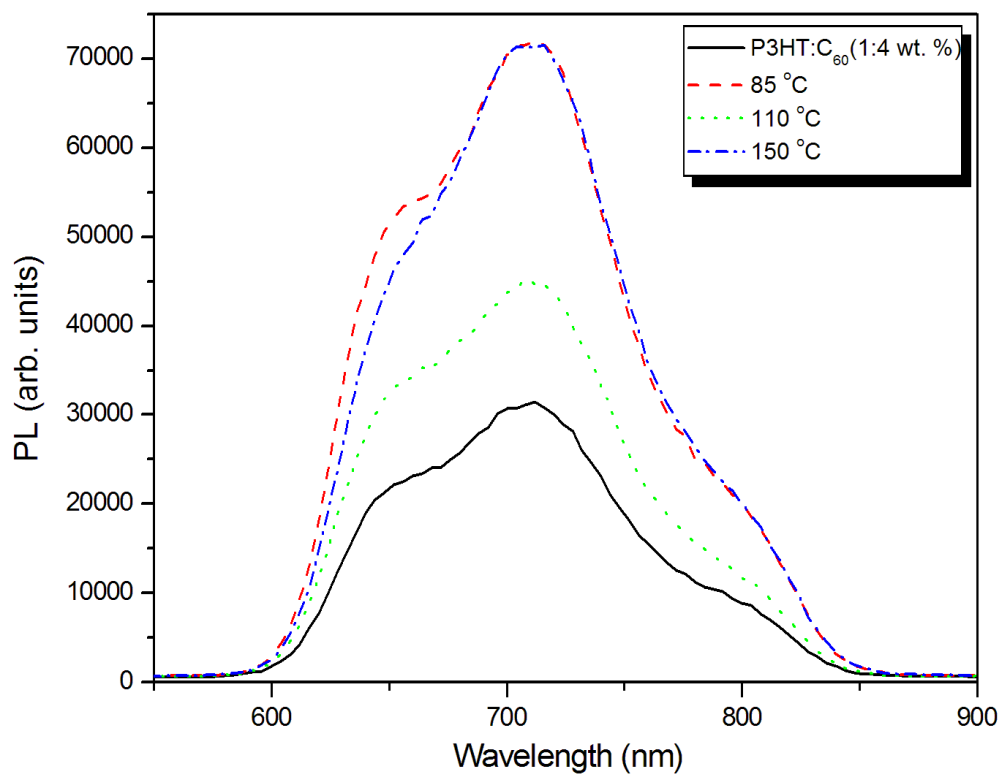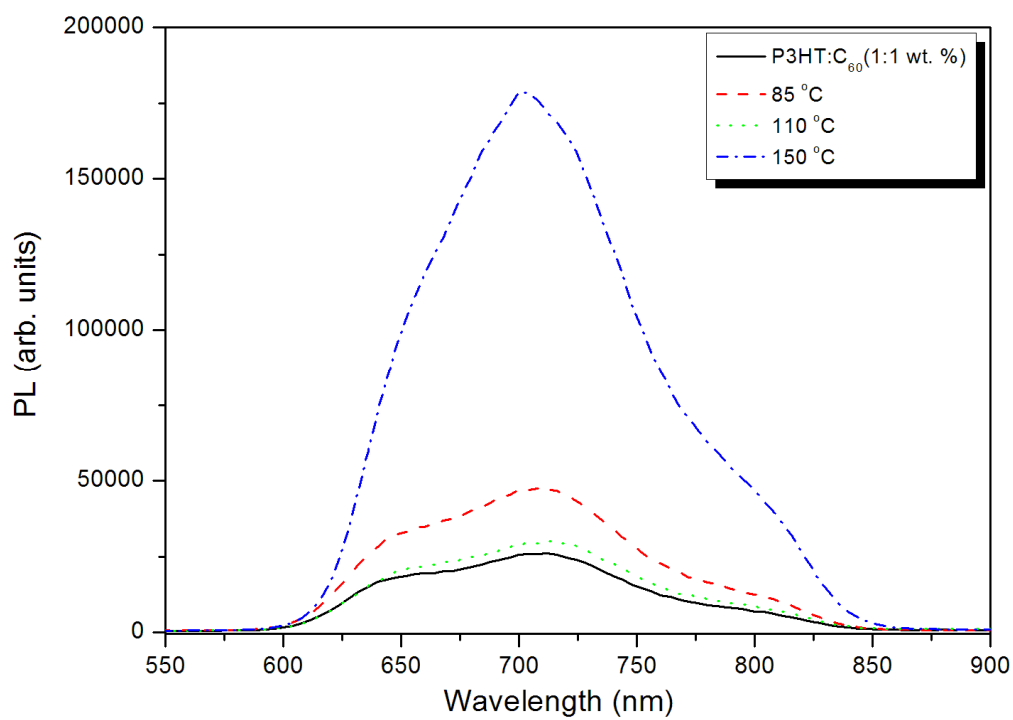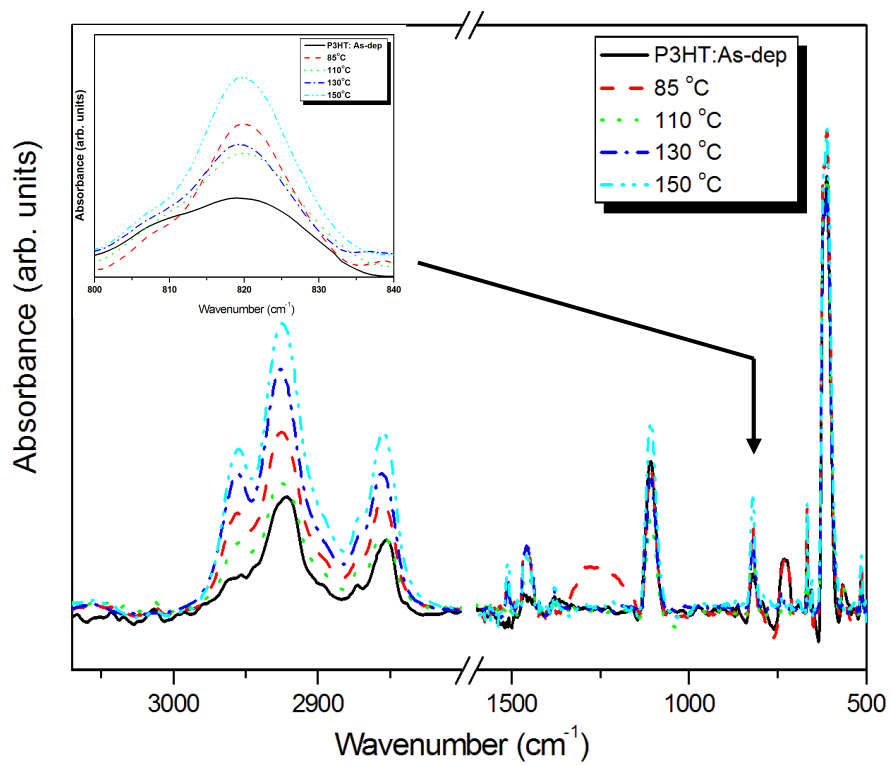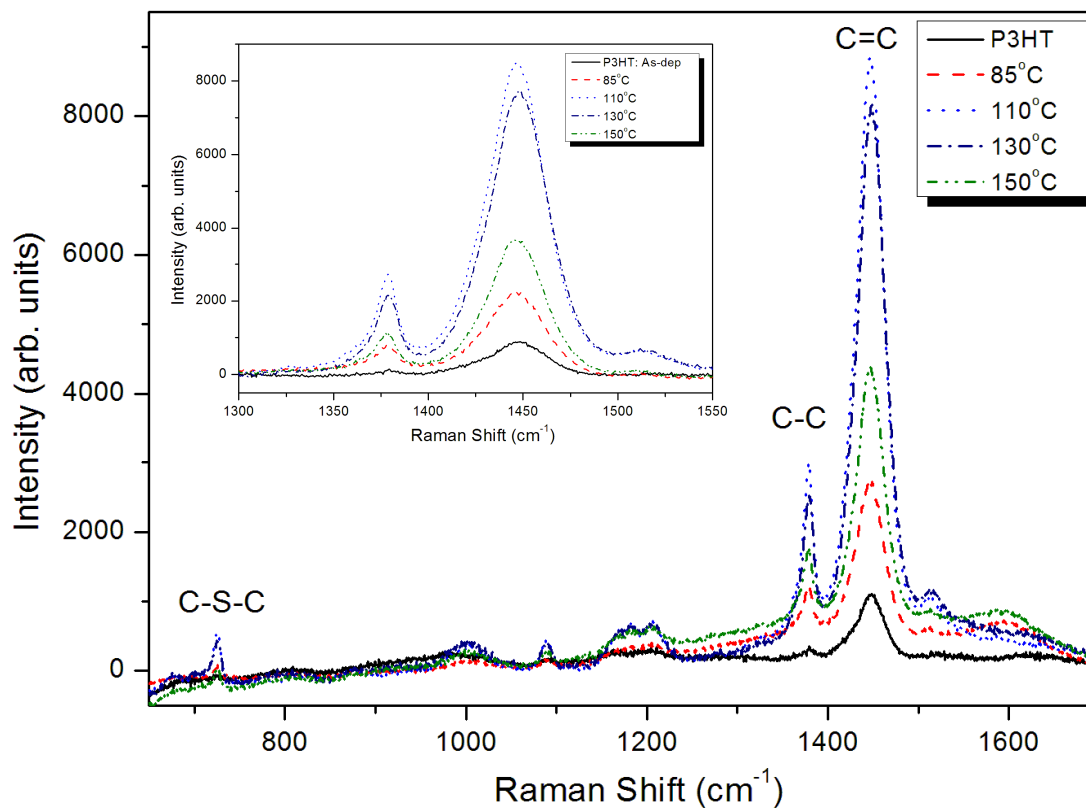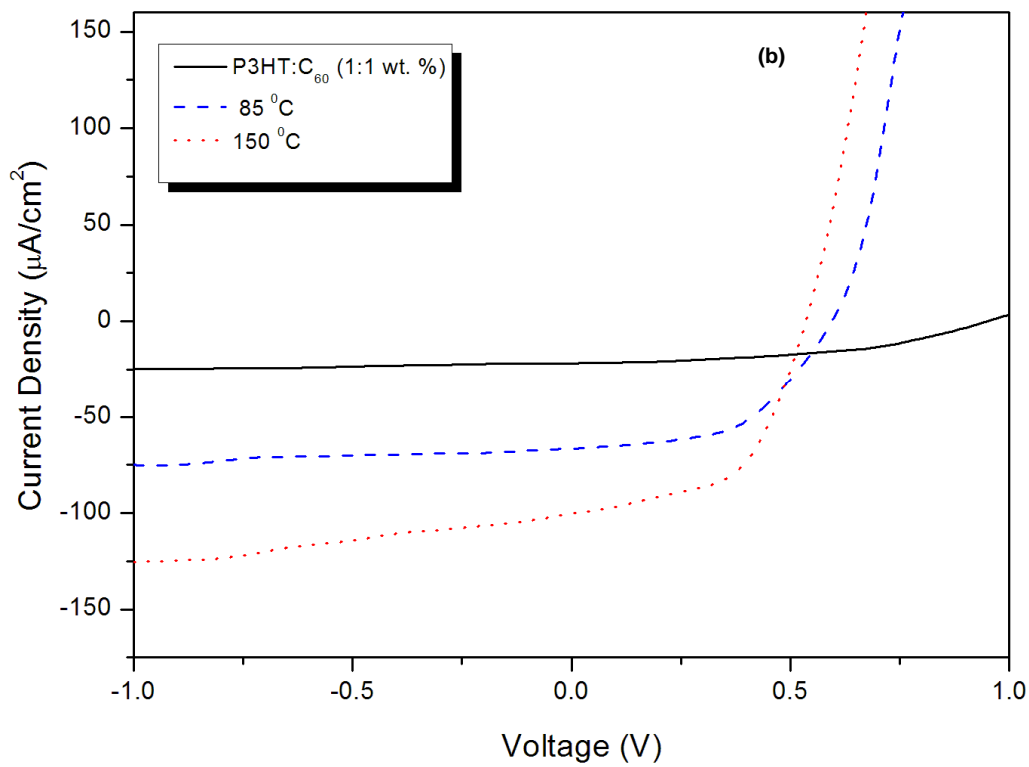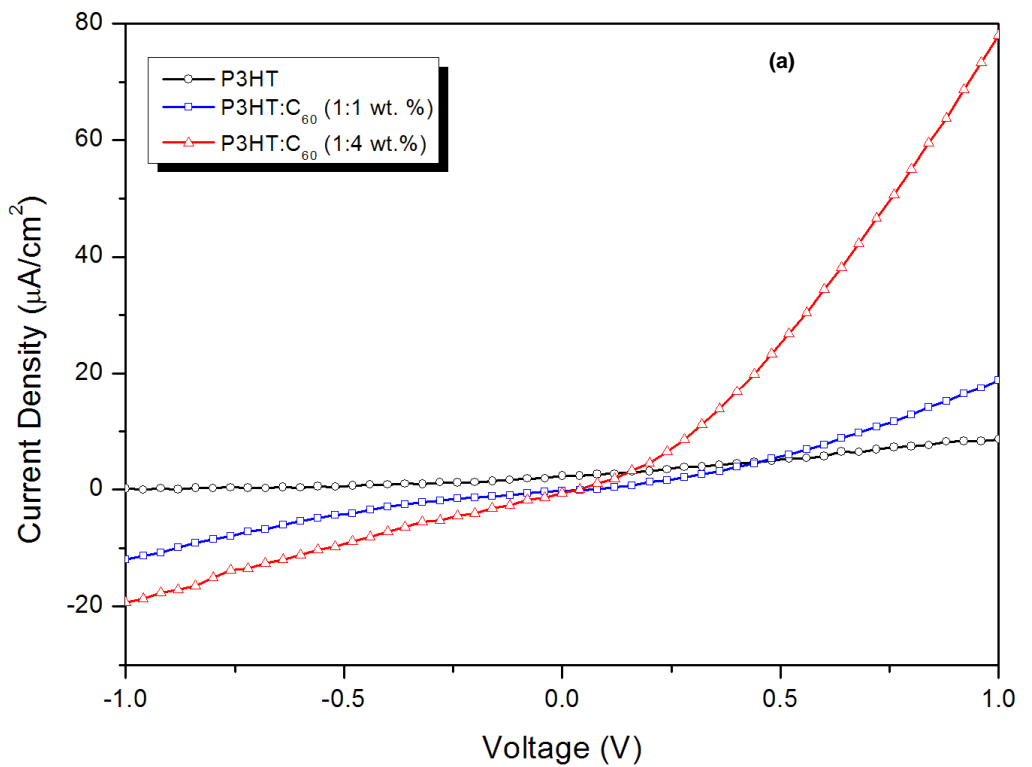
Table 1: D. Motaung et al.

Sample	C-H out of plane mode	Anti symmetric C=C stretching mode	symmetric C-C stretching mode	Aliphatic C-H stretching mode
P3HT [24,25]	819	1509	1456	2850, 2921, 2954
P3HT (85 ºC)	820	1507	1457	2856, 2925, 2955
P3HT (110 ºC)	820	1507	1457	2856, 2925, 2955
P3HT (130 ºC)	820	1507	1457	2856, 2925, 2955
P3HT (150 ºC)	820	1507	1457	2856, 2925, 2955

Device Architecture	J_{sc} ($\mu A/cm^2$)	V_{oc} (V)	FF	η (%)
Glass/ITO/P3HT:C_{60} (50 wt. %)/Al **As-prepared**	21.87	0.96	0.43	0.009
Glass/ITO/P3HT:C_{60} (50 wt. %)/Al **85 °C**	66.95	0.59	0.52	0.021
Glass/ITO/ P3HT:C_{60} (50 wt. %)/Al **150 °C**	100.1	0.54	0.54	0.029